

Binding of Endostatin to Phosphatidylserine-Containing Membranes and Formation of Amyloid-like Fibers[†]

Hongxia Zhao,[‡] Arimatti Jutila,[‡] Tuula Nurminen,[‡] Sara A. Wickström,[§] Jorma Keski-Oja,[§] and Paavo K. J. Kinnunen^{*,‡,||}

Helsinki Biophysics and Biomembrane Group, Institute of Biomedicine, University of Helsinki, Post Office Box 63 (Haartmaninkatu 8), Helsinki FIN-00014, Finland, and Departments of Pathology and Virology, Haartman Institute and Helsinki University Central Hospital, University of Helsinki, Helsinki FIN-00014, Finland

Received July 14, 2004; Revised Manuscript Received December 23, 2004

ABSTRACT: Endostatin, the 20-kDa C-terminal NC1 domain of collagen XVIII, is an endogenous inhibitor of tumor angiogenesis and tumor growth. A major problem in reconciling the many reported *in vitro* effects of endostatin is the lack of a high-affinity receptor, and a search for the latter continues. In accordance with the above, the molecular mechanisms of action of endostatin remain elusive. We show here that endostatin binds to membranes containing acidic phospholipids, phosphatidylserine (PS) or phosphatidylglycerol (PG). More specifically, a red shift in the fluorescence emission of Trp of endostatin in the presence of liposomes containing these anionic lipids was evident, revealing the average environment of Trps to become less hydrophobic. This shift was not observed for phosphatidylcholine (PC) liposomes, demonstrating the acidic lipid to be required. Quenching by endostatin of the fluorescence of a pyrene-labeled phospholipid analogue in PS containing membranes was seen, while there was no effect for PC liposomes. Resonance energy transfer from the Trp residues of endostatin to a dansyl-labeled phospholipid further confirmed the association of endostatin with PS-containing membranes, whereas there was no binding to PC liposomes. Intriguingly, the association of endostatin with PS-containing liposomes triggered the formation of fibers, with Congo red staining producing green birefringence characteristic for amyloid. Lipid was incorporated into these fibers, as shown by staining when a trace amount ($X = 0.02$) of fluorescent phospholipid analogues was present in the liposomes. No fiber formation was seen when endostatin was added to liposomes composed of PC only. Because PS has been reported to be exposed in the outer surface of the plasma membrane of cancer cells and vascular endothelial cells, our results suggest that this lipid could represent a target for endostatin in the cancer cell surface and tumors, thus suggesting a novel mechanism of its action. More specifically, analogous to a number of other cytotoxic proteins interacting with negatively charged lipids, PS-triggered fiber formation by endostatin on the surface of cancer cells would impair the permeability barrier function of the plasma membrane, resulting in cell death.

The growth of solid tumors and their metastases is dependent on angiogenesis, the formation of new capillaries from the existing microvascular system (1). This process is initiated by various cytokines and controlled by various endogenous inhibitors (1). Suppression of angiogenesis is dependent on tumor growth, providing the rationale for antiangiogenesis therapy for cancer. Endostatin is the 20-kDa NC1 domain cleaved proteolytically from the C terminus of collagen XVIII, and it has been identified as an endogenous inhibitor of tumor angiogenesis and growth (2).

Importantly, the latter activity of endostatin does not induce acquired drug resistance (3, 4), and since its initial isolation in 1997, endostatin has been the focus of intense interest, both in the clinic and laboratory. Several mechanisms have been proposed to underlie the antitumor activity of endostatin. Endostatin down-regulates vascular endothelial growth factor (VEGF)-mediated signaling (5) and induces endothelial cell apoptosis, associated with decreased levels of anti-apoptotic proteins Bcl-2 and Bcl_{X_L} (6). Endostatin also binds tropomyosin, an actin-stabilizing protein, and it has been proposed to disrupt microfilament integrity and thus trigger endothelial cell apoptosis (7). The direct effect of endostatin on cell adhesion has been proposed to be caused by suppression of integrin functions (8, 9). Endostatin can bind and inhibit matrix metalloproteinase MMP-2 (10, 11) and down-regulate the urokinase plasminogen activator system (12). It has been suggested that the arginine residues of endostatin would mediate its interaction with heparin (13, 14). However, it is not clear to what extent the above activities of endostatin contribute to its antiangiogenic and

[†] This study was supported by the Finnish Academy. Memphys is supported by the Danish National Research Council.

^{*} To whom correspondence should be addressed: Helsinki Biophysics and Biomembrane Group, Institute of Biomedicine, University of Helsinki, P.O. Box 63 (Haartmaninkatu 8), Helsinki FIN-00014, Finland. Telephone: +358-9-19125400. Fax: +358-9-19125444. E-mail: paavo.kinnunen@helsinki.fi.

[‡] Institute of Biomedicine, University of Helsinki.

[§] Haartman Institute and Helsinki University Central Hospital, University of Helsinki.

^{||} Memphys, Center for Biomembrane Physics.

antitumor effects *in vivo*. Accordingly, while the action of endostatin on tumors involves the binding of this protein to the cell surface, a major obstacle in reconciling the numerous *in vitro* effects of endostatin is the lack of an affirmative plasma-membrane receptor for this protein. A fraction of the cell-surface-bound endostatin and integrin receptor associates with lipid microdomains together with caveolin-1 (15, 16), and integrins have been suggested to regulate the overall cell-surface binding. However, the binding site(s) of the major fraction of endostatin in the cell surface could not be identified. Accordingly, the mechanisms of endostatin action remain elusive.

EXPERIMENTAL PROCEDURES

Materials. Brain phosphatidylserine (Brain PS),¹ 1-palmitoyl-2-oleoyl-*sn*-glycero-3-phosphoglycerol (POPG) and 1-stearoyl-2-oleoyl-*sn*-glycero-3-phosphocholine (SOPC) were from Avanti Polar Lipids (Alabaster, AL). 1,2-Dipalmitoyl-*sn*-glycero-3-phosphoethanol amino *N*-(5-dimethylaminonaphthalene-1-sulfonyl), triethylammonium salt (DPPDns), 1-hexadecanoyl-2-(4,4-difluoro-5-methyl-4-bora-3a,4a-diazas-indacene-3-dodecanoyl)-*sn*-glycero-3-phosphocholine (bodipy-PC), and 1-palmitoyl-2-(*N*-4-nitrobenz-2-oxa-1,3-diazol)-aminocaproyl-*sn*-glycero-3-phosphoglycerol (NBD-PG) were from Molecular Probes (Eugene, OR). 1-Palmitoyl-2-[10-(pyrene-1-yl)decanoyl]-*sn*-glycero-3-phospho-*rac*-glycerol (PPDPG) and 1-palmitoyl-2-[10-(pyrene-1-yl)decanoyl]-*sn*-glycero-3-phosphocholine (PPDPC) were from K&V Bioware (Espoo, Finland). The purity of these lipids was checked by thin-layer chromatography on silicic-acid-coated plates (Merck, Darmstadt, Germany) developed with a chloroform/methanol/water mixture (65:25:4, v/v/v). Examination of the plates after iodine staining and, when appropriate, upon UV illumination revealed no impurities. The concentrations of bodipy-PC, DPPDns, and NBD-PG were determined spectrophotometrically in ethanol using molar absorptivities ϵ_{509} of 86 000, ϵ_{336} of 4500, and ϵ_{465} of 21 000, respectively. Concentrations of the other lipids were determined gravimetrically with a high-precision electrobalance (Cahn, Cerritos, CA). Human recombinant endostatin was from Calbiochem (San Diego, CA). Congo red, magainin 2, and poly-L-lysine (polyK) were from Sigma (St. Louis, MO). Temporin L was from Tana Laboratories (Houston, TX), and indolicidin was from Bachem (Bubendorf, Switzerland). The purities of magainin 2, temporin L, and indolicidin were verified as described earlier (17, 18). The other chemicals were analytical-grade and from standard sources.

Preparation of Large Unilamellar Vesicles (LUVs). Appropriate amounts of the lipid stock solutions were mixed in chloroform to obtain the desired compositions. The solvent

was removed under a stream of nitrogen, and the lipid residue was subsequently maintained under reduced pressure for at least 2 h. The dry lipids were then hydrated at room temperature for 1 h in 20 mM Hepes and 0.1 mM ethylenediaminetetraacetic acid (EDTA) (pH 7.4). The resulting dispersions were extruded through a single polycarbonate filter (pore size of 100 nm, Millipore, Bedford, MA) using a Liposofast low-pressure homogenizer (Avestin, Ottawa, ON) to produce LUVs, with an average diameter between 111 and 117 nm (19).

Fluorescence Spectroscopy. To record lipid-induced changes in Trp emission, LUVs were added to a solution of endostatin (0.25 mM initial concentration) in 20 mM Hepes and 0.1 mM EDTA (pH 7.4), maintained at 37 °C with continuous stirring in a total initial volume of 2 mL contained in quartz cuvettes with 1 cm path length. After 15 min of equilibration, fluorescence spectra was measured with a Perkin-Elmer LS 50B spectrometer with both excitation and emission band passes set at 10 nm. Tryptophans were excited at 290 nm, and emission spectra were recorded in the range of 310–450 nm, averaging three scans. Spectra were corrected for light scattering because of vesicles. Red shifts were calculated as the difference in the center of the mass of the emission spectra. Standard deviation in the red shift was less than 0.5 nm. Fluorescence emission spectra for LUVs labeled with pyrene-containing probe PPDG ($X = 0.01$) were measured with excitation at 344 nm, and emission spectra were recorded from 360 to 500 nm, using 5 nm bandwidths for both excitation and emission. The lipid concentration used was 20 μ M. After the addition of appropriate amounts of endostatin, samples were equilibrated for 15 min before recording the spectra. Three scans were averaged, and the emission intensities at ≈ 398 and 480 nm were taken for monomer I_m and excimer I_e , respectively.

Resonance energy transfer from the Trp residues of endostatin to the dansyl chromophore in DPPDns in 40 μ M SOPC/brain PS/DPPDns (77:20:3, molar ratio) liposomes was monitored by recording dansyl emission at 510 nm with excitation at 290 nm, using 10 nm bandwidths for both excitation and emission.

Microscopy. Fibers were rapidly (within 5–10 min) formed by adding endostatin to a solution of SOPC/brain PS LUVs (8:2, molar ratio) to yield final concentrations of 0.25 mM and 100 μ M, respectively in 20 mM Hepes and 0.1 mM EDTA (pH 7.4) and were observed by phase-contrast microscopy (Olympus IX 70, Olympus Optical Co., Tokyo, Japan). The concentration for temporin L, magainin 2, and indolicidin was 1 μ M. Importantly, no fibers were seen in the absence of liposomes containing negatively charged lipids. For polarized microscopy, the fibers were incubated for 30 min with 10 μ M Congo red and their resulting birefringence was observed with the inverted microscope described above, using crossed polarizers in the excitation and emission paths.

When indicated, trace amounts ($X = 0.02$) of the fluorescent phospholipid either NBD-PG or bodipy-PC were additionally included into liposomes, and fibrils were formed as described above, imaging their fluorescence with the microscope described above equipped with a confocal scanner (Yokogawa, Tokyo, Japan) and a krypton ion laser (Melles Griot, Carlsbad, CA) as a light source, with excitation at 488 nm and a long pass emission filter (>510 nm) set

¹ Abbreviations: bodipy-PC, 1-hexadecanoyl-2-(4,4-difluoro-5-methyl-4-bora-3a,4a-diazas-indacene-3-dodecanoyl)-*sn*-glycero-3-phosphocholine; Brain PS, brain phosphatidylserine; DPPDns, 1,2-dipalmitoyl-*sn*-glycero-3-phosphoethanol amino *N*-(5-dimethylamino)-naphthalene-1-sulfonyl; LUV, large unilamellar vesicle; NBD-PG, 1-palmitoyl-2-(*N*-4-nitrobenz-2-oxa-1,3-diazol)amino-caproyl-*sn*-glycero-3-phosphoglycerol; PC, phosphatidylcholine; PG, phosphatidylglycerol; polyK, poly-L-lysine; POPG, 1-palmitoyl-2-oleoyl-*sn*-glycero-3-phosphoglycerol; PPDPC, 1-palmitoyl-2-[10-(pyrene-1-yl)decanoyl]-*sn*-glycero-3-phosphocholine; PPDPG, 1-palmitoyl-2-[10-(pyrene-1-yl)decanoyl]-*sn*-glycero-3-phospho-*rac*-glycerol; PS, phosphatidylserine; RET, resonance energy transfer; SOPC, 1-stearoyl-2-oleoyl-*sn*-glycero-3-phosphocholine.

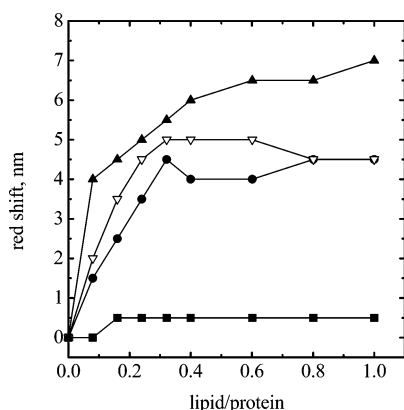


FIGURE 1: Shift of the center of mass of Trp emission spectra of endostatin (initially 0.25 mM in 20 mM Hepes and 0.1 mM EDTA at pH 7.4) recorded after the addition of the indicated amounts of liposomes composed of SPC (■), SPC/brainPS = 8:2 (mol/mol, ▲), SPC/brainPS = 6:4 (●), and SPC/POPG = 8:2 (▽). The temperature was maintained at 37 °C with a circulating waterbath.

appropriate for monitoring NBD and bodipy-PC fluorescence. Images were acquired with a B/W CCD camera (C4742-95-12 NRB, Hamamatsu Photonics K. K., Hamamatsu, Japan) interfaced with a computer, and operated by the software (AquaCosmos) provided by the camera manufacturer.

RESULTS AND DISCUSSION

The negatively charged phospholipid phosphatidylserine (PS) is expressed in the outer surface of the plasma membrane of cancer cells and vascular endothelial cells in tumors (20–22). As endostatin has a net positive charge of 5, and its 3D structure shows an extensive cationic patch involving 11 arginine residues (23). It was of interest to study whether this protein could interact with PS-containing membranes. This possibility was addressed using three different fluorescence spectroscopic assays, as follows.

Native endostatin contains four tryptophans, which are evenly distributed in its well-packed globular structure. Because the characteristics of Trp fluorescence are sensitive to changes in the environment such as those caused by alterations in the protein conformation and membrane association, for instance, we first assessed the effect of liposomes composed of the zwitterionic 1-stearoyl-2-oleoyl-*sn*-glycero-3-phosphocholine (SPC) and those of SPC and PS on the Trp emission spectra of endostatin. Importantly, a progressive red shift of the fluorescence emission from Trps was evident in the presence of membranes containing PS (Figure 1), revealing their average microenvironment becoming more polar and indicating phospholipid-induced changes in the conformation of endostatin. In contrast, virtually no changes in Trp emission were seen with SPC liposomes, thus showing the negatively charged lipid to be required for the membrane-induced changes in Trp fluorescence. Experiments with liposomes containing another negatively charged phospholipid, POPG ($X = 0.20$) instead of PS, revealed changes in the tryptophan emission of endostatin identical to those observed for PS. Accordingly, binding of endostatin to liposomes is not specific for the latter and is likely electrostatic in nature, mediated by cationic residues of the protein and the negative charges of the acidic phospholipids. For liposomes containing negatively charged

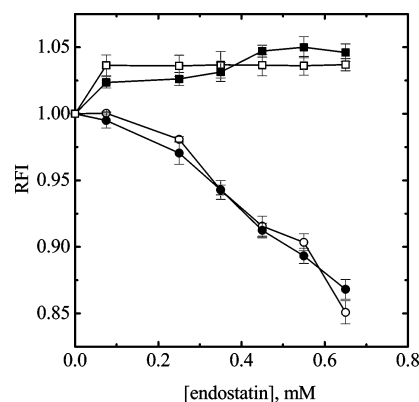


FIGURE 2: Quenching of pyrene emission from SPC/PPDPC = 98:2 (mol/mol, □ and ■) and SPC/brainPS/PPDPC = 80:18:2 (○ and ●) liposomes by the indicated concentrations of endostatin, measured at 37 °C. The initial lipid concentration was 20 μ M in 20 mM Hepes and 0.1 mM EDTA (pH 7.4). The emission intensities of pyrene monomer (□ and ○) and excimer (■ and ●) were recorded at \approx 398 and 480 nm, respectively.

lipids PS or PG ($X = 0.20$), the curves level off, indicating saturation at a lipid/protein molar ratio of approximately 1:3. This apparent stoichiometry is lower for liposomes with $X_{PS} = 0.40$ as indicated by the large red shift at lipid/protein = 0.08, followed by a less dramatic shift upon further addition of liposomes. At this higher content of PS, the behavior of the system is more complex because the observed red shift indicates further binding, although with a lower apparent affinity, up to lipid/protein = 0.60. It is also emphasized that the above molar ratios should not be understood as lipid/protein stoichiometries in the complexes formed but rather reflecting the affinities between endostatin and the lipid membranes.

The second assay assessing the interaction of endostatin with liposomes was based on the quenching of the fluorescence of a pyrene-labeled phospholipid analogue because of the membrane association of a cationic protein. More specifically, we have previously shown that the binding of cationic, membrane inserting antimicrobial peptides to liposomes causes a drastic decrease in the emission intensity of the pyrene-containing phospholipid analogue, such as PPDPC (22). Quenching of pyrene emission by these peptides could be caused by both π – π interactions between the pyrene and Trp residues as well as contacts of their cationic residues with the fluorophore resulting in a π –cation interaction (17, 18). Accordingly, to verify the association of endostatin with phospholipids, we utilized liposomes labeled with a trace amount ($X = 0.02$) of either PPDPC or PPDPC, as indicated. Progressive quenching of both pyrene monomer and excimer fluorescence emission was evident upon the addition of endostatin to PS-containing membranes, while no changes were observed for liposomes composed of SPC and PPDPC (Figure 2).

Finally, we confirmed the lipid binding of endostatin employing resonance energy transfer (RET) from its Trp residues to the dansyl-labeled lipid DPPDs (Figure 3). The observed RET readily revealed the association of endostatin with PS-containing membranes (Figure 4), while no RET was seen in the presence of phosphatidylcholine (PC) membranes.

We also studied the effect of the strongly basic polycation, polyK on the lipid association of endostatin by observing

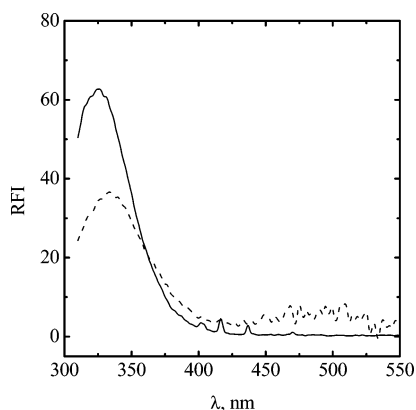


FIGURE 3: Emission spectra of 0.25 mM endostatin in 20 mM Hepes and 0.1 mM EDTA (pH 7.4) before (—) and after (---) the addition of 91 μ M SOPC/brainPS/DPPDs = 75:20:5 (mol/mol/mol) liposomes. The latter conditions correspond to lipid/protein = 0.40 (mol/mol). The spectra have been corrected for dilution and background light scattering because of liposomes. The temperature was 37 $^{\circ}$ C.

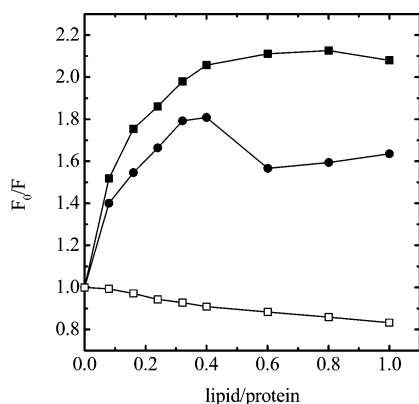


FIGURE 4: Resonance energy transfer from Trp residues of endostatin (initially 0.25 mM in 20 mM Hepes and 0.1 mM EDTA at pH 7.4) to the dansyl chromophore in SOPC/DPPDs = 97:3 (mol/mol, ●) and SOPC/brainPS/DPPDs = 75:20:5 liposomes in the absence (■) and presence of 150 mM NaCl (□). Fluorescence intensity of Trp in the range 315–335 nm was recorded after the addition of the given amounts of liposomes at 37 $^{\circ}$ C.

FRET, as described above. PolyK (0.45 μ g/mL) reversed about 10% of FRET between endostatin (4.5 μ g/mL) and SOPC/brainPS/dansyl (75/20/5) liposomes (data not shown). Under these conditions, higher concentrations of polyK caused precipitation of liposomes and strong light scattering, thus making meaningful measurements impossible. Notably, polyK mixed with liposomes before the addition of endostatin was able to block the binding as indicated by less efficient FRET. More specifically, using the same concentrations as above, there was approximately 60% less FRET from endostatin to liposomes in the presence of polyK (data not shown). This difference between polyK added before and after the addition of endostatin could reflect the virtually irreversible (under the conditions used) polymerization of the latter protein into amyloid fibers (see below). Likewise, macroscopic aggregation of polyK on the surface of anionic phospholipid-containing giant liposomes (24) would be likely to inhibit further membrane association of endostatin. No binding of endostatin to liposomes was seen in 150 mM NaCl as shown by the lack of FRET between Trp residues of endostatin and dansyl-labeled liposomes (Figure 4). These

data with polyK and NaCl, in keeping with the two acidic phospholipids PG and PS being equally effective in triggering fiber formation, emphasize the importance of the electrostatics in the interaction of endostatin with membranes containing negatively charged phospholipids. In this context, it should be noted that, in accordance with the degree of protonation of the acidic phospholipid depending on its content in the membrane (25), there are dramatic effects of ionic strength and pH on the membrane association of a cationic protein (26). These issues as well as the acidic pH in tumors are likely important when the possibility of the interactions of endostatin with PS exposed on the outer surface of cancer cells is considered (see the paragraph below). We are currently engaged in experiments aiming at high-resolution structural characterization of the fibers. These studies will also address the kinetics of their formation.

The above experiments demonstrate that endostatin interacts with bilayers containing acidic phospholipids. An obvious question is whether this interaction could be involved in the cytotoxicity of this protein. It has earlier been found that endostatin has a propensity to form amyloid fibers (27), and only the insoluble endostatin (referred to as amyloid form) but not the soluble endostatin can stimulate tissue plasminogen activator (t-PA) mediated plasminogen activation and induce cell toxicity (28). This insoluble, amyloid endostatin was found to exhibit pronounced effects on endothelial cell-mediated plasmin formation and cell adhesion (28). Interestingly, immobilized endostatin promotes and endostatin administered in solution inhibits endothelial cell migration and survival (28), suggesting that cooperative interactions of endostatin with cells are important for these activities. To this end, we have recently observed the ability of PS-containing liposomes to induce amyloid fiber formation *in vitro* by a variety of proteins involved in cancer cell killing or apoptosis, viz. lysozyme, insulin, glyceraldehyde-3-phosphate-dehydrogenase, myoglobin, transthyretin, cytochrome *c*, histone H1, and α -lactalbumin (29, 30). Interestingly, amyloid fibrils were formed also upon the binding of endostatin to PS-containing liposomes (Figure 5A), with Congo red staining of the fibers producing the characteristic birefringence (Figure 5B). Phospholipids were included in the amyloid fibers as revealed by fluorescent phospholipid analogues, such as bodipy-PC (Figure 5C). No fibers were seen in the presence of liposomes composed of PC only.

The mechanism of cytotoxicity of protein aggregates and amyloid formation is debated (31). However, it has been concluded that the amyloid itself is not cytotoxic, but it is the more microscopic aggregates preceding amyloid formation that are responsible for cell killing (32, 33). It is possible that aggregation of proteins on the membrane surface could cause rearrangement of lipids in the bilayer promoting the endocytosis of endostatin, similarly to the effects of antimicrobial peptides (17, 18) and histone H1 (29). Accordingly, PS-triggered fiber formation by endostatin could be directly related to its cytotoxicity. More specifically, PS has been reported to be exposed on the extracellular plasma membrane leaflet of cancer cells and vascular endothelial cells (20, 21). This phospholipid would thus be available for binding endostatin, resulting in the formation of toxic aggregates by the lipid-associated endostatin. Whether protein aggregation and amyloid formation are involved in the cancer cell killing by the defense mechanisms of the body is an open question.

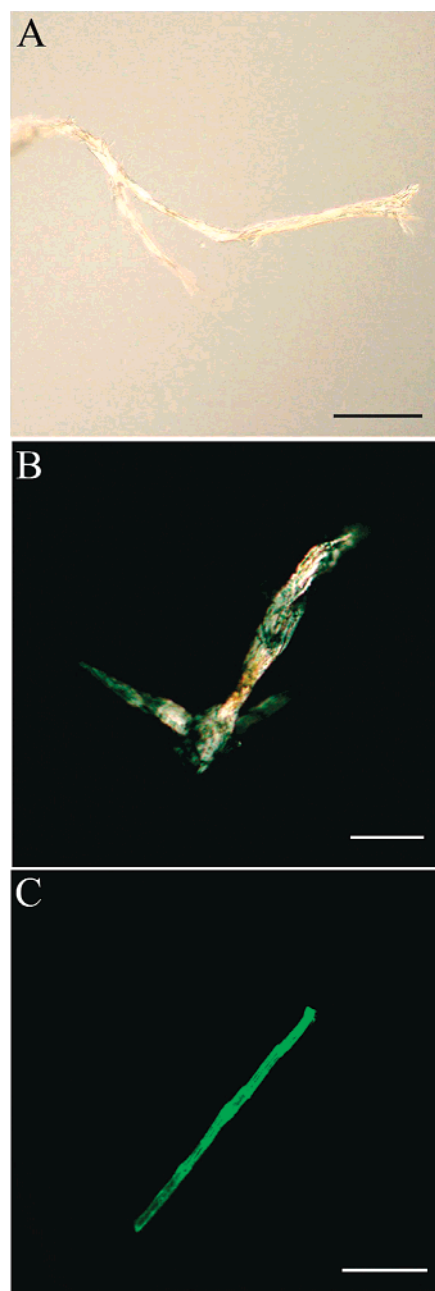


FIGURE 5: (A) Phase-contrast microscopy image of a fiber formed by endostatin in the presence of PS-containing liposomes. Endostatin and SOPC/brainPS (8:2, molar ratio) were mixed at room temperature in 20 mM Hepes and 0.1 mM EDTA (pH 7.4) to yield final concentrations of 0.25 mM and 100 μ M, respectively. (B) Fibers were formed as above and subsequently stained with Congo red (10 μ M, final concentration) and viewed under a polarizing microscope. (C) Fluorescence microscopy image of fibers formed as above except that a trace amount ($X = 0.02$) of the fluorescent phospholipid analogue bodipy-PC was additionally included in the PC/PS liposomes. Magnifications were 20 \times (A and C) and 10 \times (B). The scale bars are 5 μ m (A and C) and 6 μ m (B) in length.

However, in this context, it is of interest to note that formation of amyloid has been found in association with a wide variety of malignancies in virtually every anatomic site. Furthermore, despite their location, the cytologic appearance of amyloid was similar in all cases (34, 35). Accordingly, it is possible that proteins such as endostatin represent a defense system acting by recognizing cancer cells and vascular endothelial cells in tumors, both of which expose PS in the



FIGURE 6: Phase-contrast (left column) and polarizing microscopy after Congo red staining (right column) images of acidic phospholipid-induced fibers formed by (from top to bottom) temporin L, magainin, and indolicidin. The peptide concentration was 1 μ M, otherwise experimental conditions were as described in the caption of Figure 5.

extracellular leaflet of their plasma membranes. Interaction of endostatin with such PS-containing membranes would then induce the formation of cytotoxic protein aggregates, killing the target cell. The aggregation could, for more resistant tumors result also in the formation of amyloid deposits.

On the other hand, the lack of specificity with respect to the acidic phospholipids headgroup (i.e., PG and PS) may also relate to clinical findings, as follows. It has been observed that several antimicrobial peptides, which are at present understood to target PG in microbial membranes also kill cancer cells (for a review, see ref 36). Because the interaction of these peptides with membranes is driven by electrostatics and hydrophobicity, it seems feasible that their cytotoxicity involves the acidic PS exposed on the surface of cancer cells (20, 21). To this end, it was relevant to see if also antimicrobial, cytotoxic peptides would make Congo red staining fibers in the presence of PS-containing vesicles. Interestingly, this turned out to be the case (illustrated in Figure 6 for three cationic antimicrobial peptides temporin L, magainin 2, and indolicidin), thus suggesting similar molecular level mechanisms being responsible for the membrane permeabilization of these peptides and cytotoxic proteins in general, including endostatin. A possible mechanistic connection between fibril formation and cytotoxicity is truly intriguing and is supported by the mechanism of action suggested for lytic bacterial toxins, involving their

binding to lipid membranes and subsequent aggregation into a pore, permeabilizing the bilayer, as shown for cytolysin (37). Interestingly, it has been observed that bacterial infection in some cases results in the regression of cancer (38). While this has been attributed to be caused by tumor necrosis factor, it is also possible that it is a secondary effect of antimicrobial peptides secreted by the innate immunity system, primarily targeting the invading microorganisms.

To conclude, because (i) PS is the major acidic phospholipid exposed on the external surfaces of cancer cells and (ii) endostatin is toxic to malignant cells, we are favoring the notion that PS could indeed represent the molecular-level ligand of endostatin, making cancer cells vulnerable to this protein. However, further studies certainly are required to elucidate the importance of this interaction and the subsequent fiber formation *in vivo* inhibition of angiogenesis and tumor growth by this protein.

ACKNOWLEDGMENT

The authors thank Kristiina Söderholm and Kaija Niva for technical assistance.

REFERENCES

- Dixelius, J., Cross, M. J., Matsumoto, T., and Claesson-Welsh, L. (2003) Endostatin action and intracellular signaling: β -Catenin as a potential target? *Cancer Lett.* 196, 1–12.
- Sim, B. K., MacDonald, N. J., and Gubish, E. R. (2000) Angiogenesis and endostatin: Endogenous inhibitors of tumor growth, *Cancer Metastasis Rev.* 19, 181–190.
- Boehm, T., Folkman, J., Browder, T., and O'Reilly, M. S. (1997) Antiangiogenic therapy of experimental cancer does not induce acquired drug resistance, *Nature* 390, 404–407.
- O'Reilly, M. S., Boehm, T., Shing, Y., Fukai, N., Vasios, G., Lane, W. S., Flynn, E., Birkhead, J. R., Olsen, B. R., and Folkman, J. (1997) Endostatin: An endogenous inhibitor of angiogenesis and tumor growth, *Cell* 88, 277–285.
- Kim, Y. M., Hwang, S., Kim, Y. M., Pyun, B. J., Kim, T. Y., Lee, S. T., Gho, Y. S., and Kwon, Y. G. (2002) Endostatin blocks vascular endothelial growth factor-mediated signaling via direct interaction with KDR/Flk-1, *J. Biol. Chem.* 277, 27872–27879.
- Dhanabal, M., Ramchandran, R., Waterman, M. J., Lu, H., Knebelmann, B., Segal, M., and Sukhatme, V. P. (1999) Endostatin induces endothelial cell apoptosis, *J. Biol. Chem.* 274, 11721–11726.
- MacDonald, N. J., Shivers, W. Y., Narum, D. L., Plum, S. M., Wingard, J. N., Fuhrmann, S. R., Liang, H., Holland-Linn, J., Chen, D. H., and Sim, B. K. (2001) Endostatin binds tropomyosin. A potential modulator of the antitumor activity of endostatin, *J. Biol. Chem.* 276, 25190–25196.
- Furumatsu, T., Yamaguchi, N., Nishida, K., Kawai, A., Kunisada, T., Namba, M., Inoue, H., and Ninomiya, Y. (2002) Endostatin inhibits adhesion of endothelial cells to collagen I via $\alpha_2\beta_1$ integrin, a possible cause of prevention of chondrosarcoma growth, *J. Biochem.* 131, 619–626.
- Rehn, M., Veikkola, T., Kukk-Valdre, E., Nakamura, H., Ilmonen, M., Lombardo, C., Pihlajaniemi, T., Alitalo, K., and Vuori, K. (2001) Interaction of endostatin with integrins implicated in angiogenesis, *Proc. Natl. Acad. Sci. U.S.A.* 98, 1024–1029.
- Kim, Y. M., Jang, J. W., Lee, O. H., Yeon, J., Choi, E. Y., Kim, K. W., Lee, S. T., and Kwon, Y. G. (2000) Endostatin inhibits endothelial and tumor cellular invasion by blocking the activation and catalytic activity of matrix metalloproteinase, *Cancer Res.* 60, 5410–5413.
- Lee, S. J., Jang, J. W., Kim, Y. M., Lee, H. I., Jeon, J. Y., Kwon, Y. G., and Lee, S. T. (2002) Endostatin binds to the catalytic domain of matrix metalloproteinase-2, *FEBS Lett.* 519, 147–152.
- Wickström, S. A., Veikkola, T., Rehn, M., Pihlajaniemi, T., Alitalo, K., and Keski-Oja, J. (2001) Endostatin-induced modulation of plasminogen activation with concomitant loss of focal adhesions and actin stress fibers in cultured human endothelial cells, *Cancer Res.* 61, 6511–6516.
- Sasaki, T., Larsson, H., Kreuger, J., Salmivirta, M., Claesson-Welsh, L., Lindahl, U., Hohenester, E., and Timpl, R. (1999) Structural basis and potential role of heparin/heparin sulfate binding to the angiogenesis inhibitor endostatin, *EMBO J.* 18, 6240–6248.
- Richard-Blum, S., Feraud, O., Lortat-Jacob, H., Rencurosi, A., Fukai, N., Dkhissi, F., Vittet, D., Imbert, A., Olsen, B. R., and van der Rest, M. (2004) Characterization of endostatin binding to heparin and heparin sulfate by surface plasmon resonance and molecular modeling, *J. Biol. Chem.* 279, 2927–2936.
- Wickström, S. A., Alitalo, K., and Keski-Oja, J. (2003) Endostatin associates with lipid rafts and induces reorganization of the actin cytoskeleton via down-regulation of RhoA activity, *J. Biol. Chem.* 278, 37895–37901.
- Wickström, S. A., Alitalo, K., and Keski-Oja, J. (2002) Endostatin associates with integrin $\alpha_v\beta_1$ and caveolin-1, and activates Src via a tyrosyl phosphatase-dependent pathway in human endothelial cells, *Cancer Res.* 62, 5580–5589.
- Zhao, H., Mattila, J. P., Holopainen, J. M., and Kinnunen, P. K. J. (2001) Comparison of the membrane association of two antimicrobial peptides, magainin 2 and indolicidin, *Biophys. J.* 81, 2979–2991.
- Zhao, H., Rinaldi, A. C., Di Giulio, A., Simmaco, M., and Kinnunen, P. K. J. (2002) Interaction of the antimicrobial peptides temporins with model biomembranes. Comparison of temporin B and L, *Biochemistry* 41, 4425–4436.
- Wiedmer, S. K., Hautala, J., Holopainen, J. M., Kinnunen, P. K. J., and Riekkola, M.-L. (2001) Study on liposomes by capillary electrophoresis, *Electrophoresis* 22, 1305–1313.
- Utsugi, T., Schroit, A. J., Connor, J., Bucana, C. D., and Fidler, I. J. (1991) Elevated expression of phosphatidylserine in the outer membrane leaflet of human tumor cells and recognition by activated human blood monocytes, *Cancer Res.* 51, 3062–3066.
- Ran, S., and Thorpe, P. E. (2002) Phosphatidylserine is a marker of tumor vasculature and a potential target for cancer imaging and therapy, *Int. J. Radiat. Oncol., Biol., Phys.* 54, 1479–1484.
- Momchilova, A., Ivanova, L., Markovska, T., and Pankov, R. (2000) Stimulated nonspecific transport of phospholipids results in elevated external appearance of phosphatidylserine in *ras*-transformed fibroblasts, *Arch. Biochem. Biophys.* 381, 295–301.
- Hohenester, E., Sasaki, T., Olsen, B. R., and Timpl, R. (1998) Crystal structure of the angiogenesis inhibitor endostatin at 1.5 Å resolution, *EMBO J.* 17, 1656–1664.
- Menger, F. M. (1998) Giant vesicles: Imitating the cytological processes of cell membranes, *Acc. Chem. Res.* 31, 789–797.
- Träuble, H. (1976) Membrane electrostatics, in *Structure of Biological Membranes* (Abrahamsson, S., and Pascher, I., Eds.) pp 509–550, Plenum, New York.
- Rytömaa, M., and Kinnunen, P. K. J. (1994) Evidence for two distinct acidic phospholipid binding sites in cytochrome *c*, *J. Biol. Chem.* 269, 1770–1774.
- Kranenburg, O., Kroon-Batenburg, L. M., Reijerkerk, A., Wu, Y. P., Voest, E. E., and Gebbink, M. F. (2003) Recombinant endostatin forms amyloid fibrils that bind and are cytotoxic to murine neuroblastoma cells *in vitro*, *FEBS Lett.* 539, 149–155.
- Reijerkerk, A., Mosnier, L. O., Kranenburg, O., Bouma, B. N., Carmeliet, P., Drixler, T., Meijers, J. C. M., Voest, E. E., and Gebbink, M. F. B. G. (2003) Amyloid endostatin induces endothelial cell detachment by stimulation of the plasminogen activation system, *Mol. Cancer Res.* 1, 561–568.
- Zhao, H., Bose, S., Tuominen, E. K. J., and Kinnunen, P. K. J. (2004) Interaction of histone H1 with phospholipids and comparison of its binding to giant liposomes and human leukemic T cells, *Biochemistry* 43, 10192–10202.
- Zhao, H., Tuominen, E. K. J., and Kinnunen, P. K. J. (2004) Formation of amyloid fibers triggered by phosphatidylserine containing membranes, *Biochemistry* 43, 10302–10307.
- Dobson, C. M. (2003) Protein folding and misfolding, *Nature* 426, 884–890.
- Walsh, D. M., Klyubin, I., Fadeeva, J. V., Cullen, W. K., Anwyl, R., Wolfe, M. S., Rowan, M. J., and Selkoe, D. J. (2002) Naturally secreted oligomers of amyloid β protein potently inhibit hippocampal long-term potentiation *in vivo*, *Nature* 416, 535–539.

33. Caughey, B., and Lansbury, P. T., Jr. (2003) Protofibrils, pores, fibrils, and neurodegeneration: Separating the responsible protein aggregates from the innocent bystanders, *Annu. Rev. Neurosci.* 26, 267–298.
34. Halliday, B. E., Silverman, J. F., and Finley, J. L. (1998) Fine-needle aspiration cytology of amyloid associated with nonneoplastic and malignant lesions, *Diagn. Cytopathol.* 18, 270–275.
35. Sahoo, S., Reeves, W., and DeMay, R. M. (2003) Amyloid tumor: A clinical and cytomorphologic study, *Diagn. Cytopathol.* 28, 325–328.
36. Hancock, R. E. W., and Scott, M. G. (2000) The role of antimicrobial peptides in animal defences, *Proc. Natl. Acad. Sci. U.S.A.* 97, 8856–8861.
37. Volles, M. J., and Lansbury, P. T., Jr. (2002) Vesicle permeabilization by protofibrillar α -synuclein is sensitive to Parkinson's disease-related mutations and occurs by a pore-like mechanism, *Biochemistry* 41, 4595–4602.
38. Old, L. J. (1988) Tumor necrosis factor, *Sci. Am.* 258, 41–49.

BI048510J